15th Triennial World Congress, Barcelona, Spain

DESIGN OF A SMART MASS FLOW SENSOR FOR COMBINE HARVESTERS

K Maertens * **J De Baerdemaeker** *

* *KULeuven,Laboratory for Agro-Machinery and Processing, Kasteelpark Arenberg 30, B-3001 Leuven, Belgium, email: koen.maertens@agr.kuleuven.ac.be*

Abstract: A popular method for measuring mass flows on combine harvesters is to register the induced force on a circular chute. Since this type of sensors are strongly subjected to wear and installed on difficult accessible places, it is important to know when the sensor provides wrong measurements without interrupting the process.
In this study, a double, adaptive IIR notch filter is designed to track both resonance frequency and paddle rate of the feeding elevator on-line and providing a first rejection of both disturbance frequencies from the flow signal.

Keywords: Flow measurement, Fault detection, Signal processing, Adaptive filters

1. INTRODUCTION

Figure 1 shows two types of grain flow measurements on grain elevators mounted on combine harvesters. The first one is based on measuring the interruption

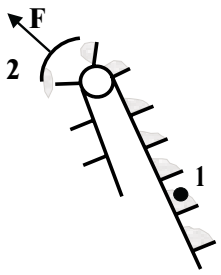

Fig. 1. Configuration of grain flow measurements on a grain elevator: 1, volumetric flow measurement; 2, mass flow measurement

time of an optical beam, transmitted through the grain elevator. Longer dark times imply higher volumetric flows. After reckoning with the volumetric weight, a mass flow measurement is achieved. Since volumetric weight is difficult to measure and has important within field variations, no accurate results are achieved. Therefore, the use of a mechanical flow measurement is preferred since a mass flow is directly achieved, independent on the properties of passing material(Strubbe 1997). This type of configuration is widely used for purposes of yield mapping systems and automatic tuning systems for combines.

Figure 2 shows a typical example of a measured mass flow signal. Two large peaks are visible on the frequency spectrum. One peak at $11.6Hz$ corresponds with the resonance frequency of the sensor, a second one at $13.2Hz$ corresponds with the paddle rate of the grain elevator. Both frequencies are strongly disturbing the flow signal but contain important information about the working status of the sensor.

To use the measured flow signal, an appropriate filter must be designed. Since the signal contains interesting information about the working status of the combine harvester and local grain yield, the frequency content up to $5Hz$ should stay unchanged. When both disturbance frequencies stay constant in time, a fixed double notch filter can be used as pre-filter for a low pass *Butterworth* anti-aliasing filter.

Due to variations of elevator speed or wear on the circular chute, both disturbances vary in time. Therefore, an automated design procedure for a robust, double notch filter is developed. Besides, an adaptive algorithm must be introduced to put both notch frequencies

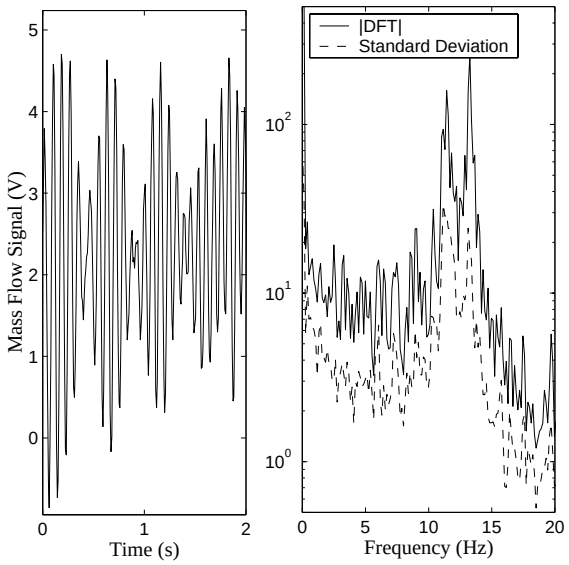

Fig. 2. Signal properties of mechanical mass flow measurement

on their corresponding disturbance frequency. To keep the physical interpretation of both notch frequencies, the same notch must be placed on the same disturbance under all measurement conditions.

2. DESIGN OF MULTIPLE NOTCH FILTER

The ideal notch filter $F_{notch}(j\omega)$ can be defined by

$$F_{notch}(j\omega) = \begin{cases} 0, \ \omega = \omega_i \\ 1, \ \omega \neq \omega_i \end{cases} \tag{1}$$

where $\{\omega_i\}$ are denoting the different notch frequencies. The standard way to approximate the ideal notch characteristic is given by

$$F(z^{-1}) = \frac{N(z^{-1})}{N((z/\rho)^{-1})} \quad (0 \ll \rho < 1) \tag{2}$$

Numerator $N(z^{-1})$ places zeros on the unit circle accordingly to each notch frequency $\{\omega_i\}$. Two poles are put on the the same frequency lines but with range ρ. This parameter defines the gain and 3-dB bandwidth B (Hz). For low 3-dB bandwidths and by this, poles near the unit circle, numerical problems can arise when different single notch filters are placed in cascade.

In Regalia *et al.* (1988) an alternative approach is formulated based on a combination of all-pass filters:

$$F(z^{-1}) = 0.5\left\{1 + A_{2N}(z^{-1})\right\} \tag{3}$$

All-pass filter $A_{2N}(z^{-1})$ of $2N$-th order is determined by a cascade of second-order all-pass filters (fig.3):

$$A_{2N}(z^{-1}) = \prod_{i=1}^{N} \frac{\sin\theta_{2i} + \sin\theta_{1i}(1+\sin\theta_{2i})z^{-1} + z^{-2}}{1 + \sin\theta_{1i}(1+\sin\theta_{2i})z^{-1} + \sin\theta_{2i}z^{-2}} \tag{4}$$

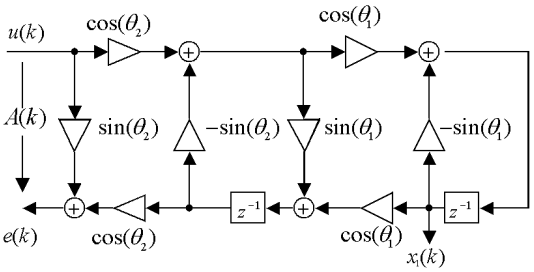

Fig. 3. Normalized second order lattice filter

The individual notch parameters $\{\theta_{1i}\}$ and $\{\theta_{2i}\}$ are respectively defined by [1]

$$\theta_{1i} = \omega_i - \pi/2 \tag{5}$$

$$\sin(\theta_{2i}) = \frac{1 - \tan(B_i/2)}{1 + \tan(B_i/2)} \tag{6}$$

3. SINGLE ADAPTIVE NOTCH FILTER

From equation 5, parameters $\{\theta_{1i}\}$ are directly related with the frequency of the sinusoidal disturbances. Since these frequencies are time-varying, an adaptive algorithm must be introduced.

To tune frequency parameter θ_1, following algorithm is proposed by Regalia (1991):

$$\theta_1(k+1) = \theta_1(k) - \mu(k)e(k)x_1(k) \tag{7}$$

with $\mu(k)$ a positive gain sequence, $e(k)$ and $x_1(k)$ respectively the output and regressor signal of figure 3. Different choices can be made for gain sequence $\mu(k)$. Here, the gain sequence is kept constant. A larger gain constant will result in a higher capability for tracking frequency variations. A lower gain will produce a frequency estimator with lower variance.

Assume the flow signal can be approximated by set of sinusoidal signals in addition to a white noise sequence $\nu(k)$.

$$u(k) = \nu(k) + \sum_{i=1}^{M} a_i cos(\omega_i k + \phi_i) \tag{8}$$

For the continuous equivalent, the frequency tracking dynamics for M sinusoidal disturbances can be approximated by (Regalia 1991):

$$\frac{d\theta_1(\tau)}{d\tau} = -\sum_{i=1}^{M} \frac{a_i^2}{4\pi} \frac{\cos\theta_1(\tau)\cos\theta_2}{|D(e^{-j\omega_i}, \Theta(\tau))|^2} (\cos\omega_i + sin\theta_1(\tau)) \tag{9}$$

$$= -\beta(\Theta(\tau)) \left[\sin\theta_1(\tau) + \sum_{i=1}^{M} c_i(\Theta(\tau))\cos\omega_i\right] \tag{10}$$

[1] Frequencies and bandwidths are normalized between 0 and 2π

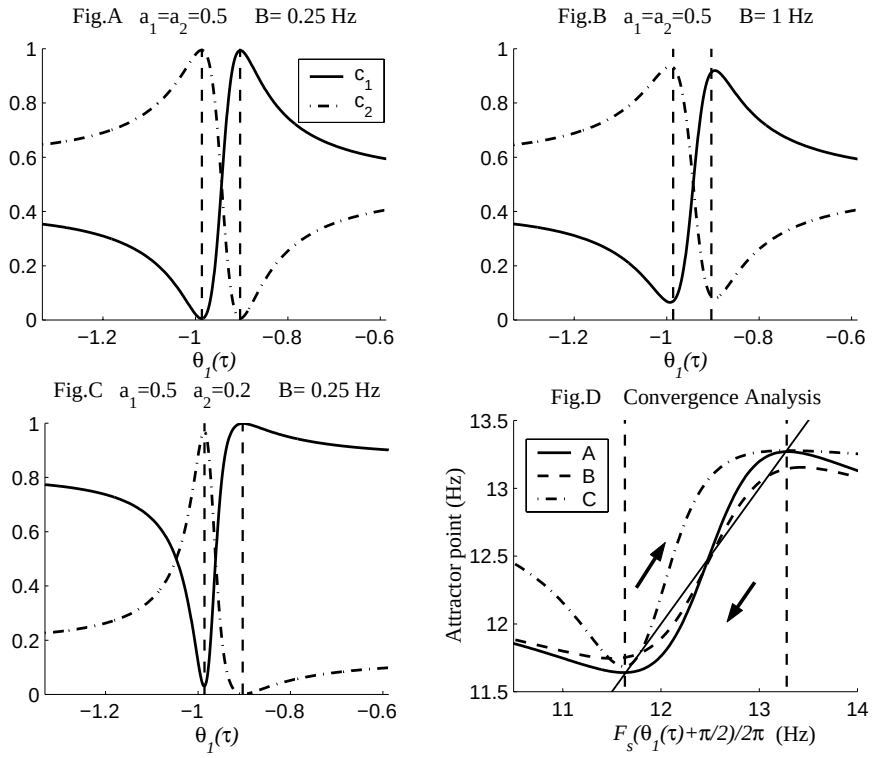

Fig. 4. Convergence analysis of single adaptive notch filter with two sinusoidal disturbances. Figures A, B and C are illustrating the influence of amplitudes $\{a_i\}$ and bandwidth B on $c_i(\Theta(\tau))$-weights. Figure D shows the relation between the instantaneous frequency estimation and the corresponding attractor frequency.

where parameters β and c_i are strongly nonlinear in function of parameter matrix $\Theta(\tau)$, a time-varying matrix composed of $\{\theta_{1i}(\tau), \theta_{2i}\}$.

$$\beta(\Theta(\tau)) = \sum_{i=1}^{M} \frac{\cos\theta_2 \cos\theta_1(\tau) a_i^2}{4\pi |D(e^{-j\omega_i}, \Theta(\tau))|^2} \qquad (11)$$

$$c_i(\Theta(\tau)) = \frac{a_i^2 / |D(e^{-j\omega_i}, \Theta(\tau))|^2}{\sum_{l=1}^{M} a_l^2 / |D(e^{-j\omega_l}, \Theta(\tau))|^2} \qquad (12)$$

Denominator $D(z^{-1}, \Theta(\tau))$ corresponds with the denominator of a single all-pass filter given by equation 4 (N=1). Since $\beta(\tau)$ is strictly positive in normal conditions ($|\theta_1(\tau)| < \pi/2$ and $|\theta_2(\tau)| < \pi/2$), the instantaneous attractor point is defined by the second term of eq. (10). Parameters c_i are strictly positive under all conditions.

Studies based on the design of appropriate *Lyapunov* functions (Regalia 1991, Bodson and Douglas 1997) have proven the existence of local attractor points near each frequency ω_i in case of a small bandwidth B. Once the system has reached the neighborhood of one attractor point, stability is guaranteed in case of smooth frequency variations.

Figure 4 illustrates this behaviour for two ($M = 2$) sinusoidal disturbances corresponding with the measured grain flow signal of Fig. 2. The disturbance frequencies are situated at 11.6 and 13.2 Hz. Figures A, B and C show the variations of the c_i-weights in function of $\theta_1(\tau)$ for different disturbance amplitudes and notch bandwidth B. The position of the instantaneous attractor point $F_a(\tau)$(Hz) is plotted in figure D and calculated by means of

$$F_a(\tau) = \frac{F_s}{2\pi}\left[\arcsin\left(-\sum_{i=1}^{2} c_i(\tau)\cos\omega_i\right) + \pi/2\right] \qquad (13)$$

Three curves corresponding with the configuration of figures A,B and C are compared in figure D. A solid line is drawn to separate the direction of attraction. Points on curves in the upper-left corner correspond with a positive $d\theta_1(\tau)/d\tau$ (eq.10) and by this, result in increasing frequency estimates. Points in the bottom-right corner bring about decreasing frequency estimations. Parameter-values are transformed into frequency units (Hz) to simplify physical interpretation.

- In case bandwidth B is large in relation with the difference between both disturbance frequencies, the c_i-coefficients do not become perfectly one (fig.B) at ω_i, resulting in a biased frequency estimation (fig.D).
- The presence of a strong sinusoidal disturbance in the immediate neighborhood of the aimed one, introduces problems of convergence and bias-terms(fig.C,D). In the case of configuration C, a slight perturbation of the θ_1-estimation around the weak frequency will let the tracking algorithm converge towards the other, stronger frequency (fig.D).Once the other disturbance fre-

quency is tracked, only exceptional disturbances will bring the tracking algorithm back to the original one.

Since all figures are based on a continuous approximation of the discrete algorithm, no gain sequences appear in the dynamic relations. To implement this techniques, a gain sequence μ (eq.7) has to be chosen. A low gain will make the system variations slower, introducing possible wrong trackings in case of fast variations of one of the disturbance frequencies. A high gain will make the tracking algorithm more nervous and by this, more sensitive for perturbations in case of a high white noise variance σ_v^2 (eq.8).

4. DOUBLE ADAPTIVE NOTCH FILTER

The measured flow spectrum of Fig.2 illustrates how both disturbance frequencies are situated close to each other and have about the same energy. The convergence analysis of Fig.4 has shown the difficulties to track one specific frequency. When one disturbance frequency is reduced before the other one is tracked, a more robust algorithm is found.

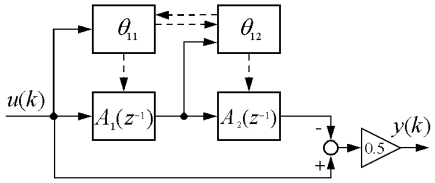

Fig. 5. Bidirectional parameter flow, realizing a robust, double adaptive notch filter

Figure 5 illustrates how latter improvement for robustness can be guaranteed in case of two disturbances, by means of a bidirectional connection between both tracking algorithms. The cascaded connection of Regalia (1991) induces parameter $\theta_{12}(k+1)$ to follow the weaker paddle rate after the stronger resonance frequency is filtered out by means of a first notch filter. In this configuration, an analogous correction is added in the other direction where the previous estimated $\theta_{12}(k)$ is used to filter the input signal before the actual $\theta_{11}(k+1)$-estimation.

4.1 *Tracking results*

To analyze the tracking capability of the algorithm, simulations are performed in *Matlab*. As input signal, two disturbance frequencies are generated with nominal frequencies of 13.2 and 11.6 Hz and amplitudes of respectively 0.5 and 0.27. Gaussian white noise is added with a power spectrum of -10 dB. Bandwidths B_i are set on 0.5 Hz and each simulation is initialized with $\theta_{11}(0)$- and $\theta_{12}(0)$-values corresponding with intial frequencies of 14.5 and 10.5*Hz*. Gain sequence μ_1 of the θ_{11}-estimator is set at a constant value of

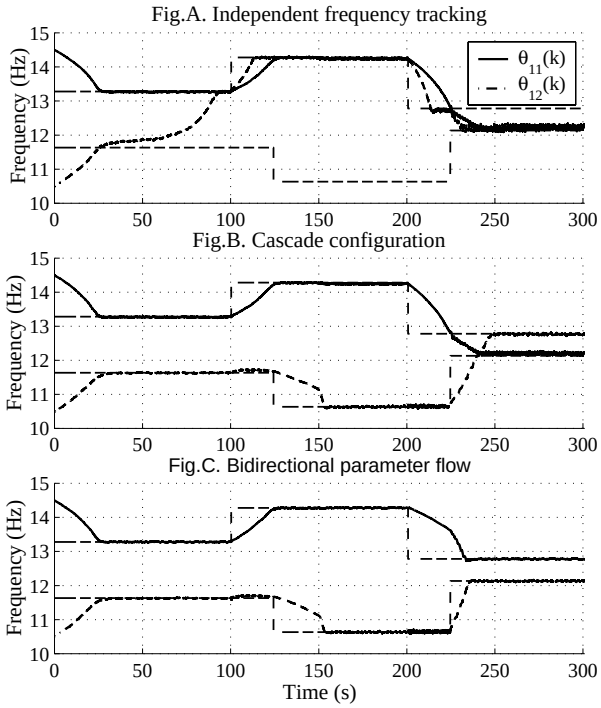

Fig. 6. Simulation results for three different realization of a double notch filter: fig.A, two independent frequency estimators; fig.B, unidirectional cascade configuration (Regalia 1991); fig.C, bidirectional parameter correction (fig.5)

$0.5\ 10^{-4}$. Gain μ_2 is set at a constant value of 10^{-5}. Simulations are carried out at a sample rate of 125*Hz*.

Figure 6 shows the results of three double adaptive notch filters. Each disturbance frequency varies two times. At 150 seconds, the amplitude of the paddle rate disturbance is amplified with a factor 2.5 and becomes stronger than the resonance frequency. The three plots of figure 6 correspond with following configurations:

(1) Two tracking algorithms are estimating the frequencies independently. The resulting $\{\theta_{1i}(k)\}$ and $\{\theta_{2i}\}$ are implemented in the adaptive allpass filter of equation 4 and applied to the input signal.

As could be expected from the stability analysis of figure 4D, no stable tracker for the weaker paddle rate frequency is found. Already at the initialization of the notch filter, the second frequency estimator converges towards the strongest frequency. After time step 150, the stronger paddle rate is followed by both frequency trackers. After time step 150, a bias term arises on both tracking algorithms due to the nearby paddle rate disturbance.

(2) As proposed by Regalia (1991), the strongest disturbance ω_1 is estimated first. Subsequently, a second order notch filter is placed and the second disturbance frequency ω_2 is estimated.

During the first part of the simulation, both frequency estimators converge consistently to the effective disturbance frequencies of the system.

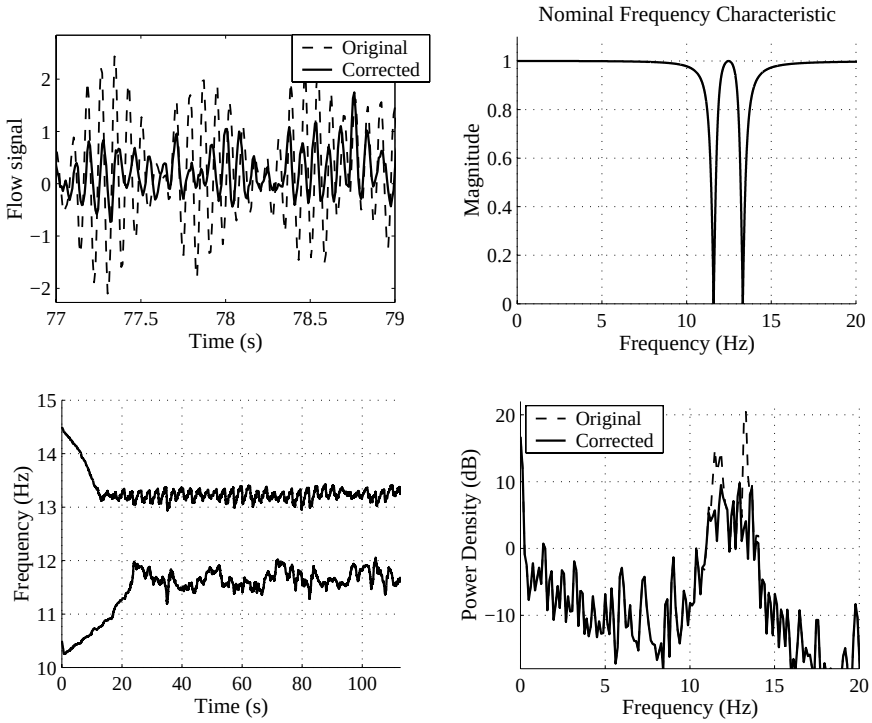

Fig. 7. The tracking and filtering results by applying the bidirectional, double adaptive notch filter on a measured grain flow signal

As long as the power of resonance frequency dominates the paddle rate, no problems arise. After time step 150, the θ_{11}-estimation keeps following the strongest with a small bias term. The θ_{12}-tracker follows consistently the weakest disturbance. Again, a bias term arises on the resonance frequency estimation due to the weak neighboring paddle rate.

(3) The bidirectional parameter flow configuration of figure 5 is used. The interesting properties of the single adaptive notch filter are approximated for both frequency estimations without bias terms or instabilities.

4.2 *Filter results*

The configuration of Fig.5 is applied on effective measured grain flow signals with the settings and initialization of previous simulation. The results in time- and frequency domain are shown in figure 7 together with the estimated frequencies and a nominal frequency characteristic (notch on 11.6 and 13.2 Hz). As well in time-domain as in frequency domain, the influence of the adaptive notch filter on the measured signal is clearly visible. Since the grain flow signal does not exhibit a constant power spectrum outside the disturbance frequencies, some low frequency ripples are present in the frequency trajectories.

The largest peak is decreased with 10dB. As result, a fixed second order *Butterworth* filter can be used to register the grain flow at a sample rate of 5Hz, ready for precision farming purposes(Maertens *et al.* 2001).

A closer look at the low frequency content ($< 5Hz$) reveals other peaks which are also interpretable. After removing the frequency content due to the paddle rate and resonance frequency, a similar approach can be used to track these peaks.

5. CONCLUSIONS

Grain flow is an important parameter to know for purposes of yield mapping and automatic tuning systems. To guarantee a stable and robust working of latter systems, it is important to have continuously, quantitative information about the state if this measurement device. When wrong measurements are provided, a signal should be given to these systems. In this correspondence, a method is presented to track two important disturbance frequencies in the measured flow signal: the resonance frequency of the sensor provides information about the dynamic status of the sensor and the paddle rate describes the dynamic properties of the entering grain flow.

The method is based on a robust, double adaptive IIR notch filter. By using precedent estimations of the disturbance frequencies, a bidirectional parameter flow can be designed, resulting in a robust, accurate and stable estimation of both frequencies. In case of more disturbance frequencies, the extension is straightforward. Next to the interesting tracking properties, this algorithm is computationally cheap since it is composed of a sequential algebraic correction equation (eq.7) and filter design (fig.3). By this, a smart flow

sensor is achieved without extra hardware cost and with negligible software additions.

ACKNOWLEDGEMENTS

The authors gratefully acknowledge the I.W.T. (Instituut voor Wetenschappelijk Technologisch onderzoek) for the financial support through doctoral grant No.001249. This study has been made possible through cooperation of New Holland Belgium.

6. REFERENCES

Bodson, M. and S.C. Douglas (1997). Adaptive algorithm for the rejection of sinusoidal disturbances. *Automatica* **33**(12), pp.2213–2221.

Maertens, K., J. De Baerdemaeker, H. Ramon and R. De Keyser (2001). An analytical grain flow for a combine harvester. part 2: Analysis and application of the model. *J. of Agr. Eng. Res.* **79**(2), pp.187–193.

Regalia, P.A. (1991). An improved lattice-based adaptive iir notch filter. *IEEE Trans. Signal Proc.* **39**(9), pp.2124–2128.

Regalia, P.A., K. Mitra and P.P. Vaidyanathan (1988). The digital all-pass filter: A versatile signal processing building block. *Proc. IEEE* **76**, pp.19–37.

Strubbe, G. (1997). Mechanics of friction compensation in mass flow measurements of bulk solids. PhD thesis. Dept. of Mechanical Engineering, KULeuven.